Hindawi
Advances in Civil Engineering
Volume 2023, Article ID 4575118, 11 pages
https://doi.org/10.1155/2023/4575118

Research Article

Numerical Study of the Influence of the Spatial Distribution of Oversized Rock Blocks on the Stability of Soil-Rock Mixture Slopes

Wenwei Gao,[1] **Hairong Yang**,[2] **JinBiao Teng**,[1] **and Yongshuai Sun**[3]

[1]*Department of Architecture and Engineering, Yan'an University, Yan'an 716000, China*
[2]*Institute of Language Literature and Mass Media, Yan'an University, Yan'an 716000, China*
[3]*College of Water Resources & Civil Engineering, China Agricultural University, Beijing 100083, China*

Correspondence should be addressed to Wenwei Gao; gaowwan@163.com

Received 20 December 2022; Revised 7 March 2023; Accepted 8 March 2023; Published 19 May 2023

Academic Editor: Jian Ji

Soil-rock mixtures (S-RMs), as special engineering geological materials, are widely distributed in mountainous regions and are important hosts of slope disasters. Stability studies are very important for predicting S-RM slope safety during the construction and operation of engineering projects. To investigate S-RM slope stability considering the spatial distribution of oversized rock blocks in the slope, the distinct element method (DEM) program particle flow code in two dimensions (PFC^{2D}) was used to analyse the stability of slopes composed of S-RMs. First, according to the stochastic approach, different numerical models of an S-RM slope were established with different oversized rock block spatial distributions. Then, the S-RM slope models were simulated, the safety factor and sliding characteristics of the slopes were analysed, and the unbalanced contact force and rotational characteristics of the oversized rock blocks were discussed. Finally, the concept of key rock blocks in S-RM slopes was proposed, and their spatial distribution characteristics and influence characteristics were summarized. The findings of this study suggest that oversized rock blocks have a certain influence on the stability of S-RM slopes.

1. Introduction

Soil-rock mixtures (S-RMs), such as colluvium, eluvium, and diluvium that were formed in the Quaternary, are composed of rock blocks and soil and are a special engineering geological body, since they have the characteristics of poor consolidation, low strength, complex geotechnical structure, and strong water sensitivity [1, 2]. Because of the complex material composition and structure of an S-RM, it is difficult to accurately grasp the corresponding geological model and medium characteristics, as its mechanical properties are greatly affected by its complex internal structure and composition; however, landslide disasters commonly occur in S-RM slopes [3]. At present, in engineering construction, an S-RM slope is generally classified as a special soil slope according to its coarse-grained material characteristics and is obviously only suitable for relatively conservative situations or only for situations in which rock blocks have little impact [4]. For example, when the rock proportion of a slope is greater than 60%, the corresponding factor of safety is largely enhanced [5], and it is necessary to consider the long-axis inclination angles of rocks in estimating S-RM slope stability [6]. However, when the impact of rock blocks is large, it will inevitably cause large construction errors and slope safety issues [7, 8].

During the last three decades, many researchers have studied the physical and mechanical properties of S-RMs with various methods [9–12]. Such studies have mainly focused on the effects of rock block structure characteristics, such as rock block proportion (RBP) [13–15], number of rock block edges [5, 16], rock block aspect ratio [17, 18], rock block size distribution [19, 20], and rock block orientation [21–23], on the physical and mechanical properties of S-RMs, and many research results have been obtained. In recent years, with the development of computer technology and computed tomography (CT) technology, the failure of soil rock mesoscopic structures has also become a hot topic in S-RM research [24, 25]. The influence of the spatial

distribution of the rock blocks on the mechanical properties of an S-RM has rarely been considered in previous studies. From the aspects of the geological origin and rock block structure, S-RMs have various geneses and structures, which lead to poor sorting and high randomness of the rock blocks in the S-RMs [26]. However, due to long-distance transportation and slow deposition, the rock blocks in S-RM slopes of different origins have different spatial distributions [27] and different effects on slope deformation and failure [28, 29]. In addition, research has shown that oversized rock blocks are very common in S-RMs (Figure 1), and the spatial distribution of oversized rock blocks is difficult to incorporate into the study of S-RMs [30]. Therefore, it is of great significance to study the spatial distribution of oversized rock blocks and their influence on the mechanical properties and deformation and failure of S-RM slopes to improve the theoretical study of S-RM slopes and the prevention and control of related geological disasters, such as S-RM landslides.

Accordingly, the main goal of this study was to investigate slope stability considering the spatial distribution of oversized rock blocks. A distinct element method (DEM) program, particle flow code in two dimensions (PFC^{2D}), was used to analyse the stability of slopes composed of S-RMs. First, according to the stochastic approach, different numerical models of S-RM slopes were established with different spatial distributions of rock blocks. Then, the S-RM slopes were simulated, the safety factor and sliding characteristics of the slopes were analysed under the influence of oversized rock blocks, and the unbalanced contact force rotational characteristics of the oversized rock blocks were discussed. Finally, the concept of key rock blocks in S-RM slopes was proposed, and their spatial distribution characteristics and influence characteristics were summarized.

2. Setup of the Slope Numerical Model

2.1. Generation of Irregular Rock Blocks. Because rock shape is one of the main factors affecting the mechanical behaviour of S-RMs, it is necessary to model rock blocks with high accuracy. PFC^{2D} provides a clump command for simulating irregular blocks [31]. A clump is a rigid collection of rigid spherical pebbles; the surface is defined by the pebble positions and radii, and the surface properties can be specified independently for each pebble. Meanwhile, the clump is a typical rigid body, and the particles in contact with the clump are not affected by its internal structure in the calculation. The particles do have a certain contact relationship with the pebbles constituting the clump boundary [32]. Therefore, no matter how large the external force acting on it, the clump is not damaged. Therefore, this paper uses clumping to simulate the undeformed rock blocks [33].

At present, the Monte Carlo method is the most widely used method for the generation of random structural rock blocks [34], and the basic process is as follows: ① the parameters of the rock blocks in an S-RM slope are obtained by means of exploration, and the statistics of the different shapes of rock blocks are input; ② the correlation law of rock block shape characteristics is analysed, the statistical model is established, and the values of the rock block shape parameters are determined according to random sampling results; and ③ according to the shape parameters of the rock blocks and the secondary development of PFC^{2D}, a random rock block model is established. Detailed information regarding the generation algorithm used in this paper can be found in Wang et al. [35].

2.2. Calibration of Microscopic Parameters. After the establishment of the model, it is necessary to select appropriate microscopic parameters to reflect the macroscopic parameters of the rock and soil mass in PFC^{2D}. Research results have shown that the particle contact bonding model can better reflect the mechanical behaviour of soil [36]. In the contact bonding model, the material mesoscopic parameters are mainly the particle density ρ, maximum particle radius $R_{\max}$ (the particle radius follows a uniform distribution), ratio of maximum particle radius to minimum particle radius $R_{\max}/R_{\min}$, normal contact stiffness between particles k_n, normal-to-shear stiffness ratio k_n/k_s, tensile strength of particle bonding F_t^c, shear strength of particle bonding F_s^c, and friction coefficient (ball-ball/ball-rock) μ [37]. When the particle size range is certain, the deformation modulus of the material is related to the particle normal contact stiffness, Poisson's ratio of the material is related to the particle contact stiffness ratio, and the elastic modulus and strength of the material are related to the bonding parameters and particle friction coefficient. Based on the analysis of particle parameters, the ultimate mesoscopic mechanical parameters of the soil particles used in this paper are listed in Table 1 [33]; additionally, the density of the rock block is $2700\,kg/m^3$, and the local damping coefficient is set as 0.5 to dissipate energy.

2.3. Reduced Strength Method in PFC^{2D}. Stability analysis is one of the important factors in landslide research [38], and the safety factor of a slope is the quantitative description of the current stable state of the slope. At present, the slope stability research method is relatively mature [39, 40], and the safety factor is usually calculated by the strength reduction method, which gradually reduces the strength parameters of the soil in numerical calculations until it reaches the failure state [28]. In the discrete element method, the mechanical parameters of soil are characterized by the bonding strength parameters between mesoscopic particles by reducing the friction coefficient between particles (μ) and connection strength cb to solve the stability coefficient of the slope and achieve optimal results [5]. In the PFC^{2D} calculation, as the friction coefficient μ and the particle connection strength cb (tensile strength and shear strength) decrease, there must be critical values of μ_{cr} and cb_{cr}, when $\mu \le \mu_{cr}$ and $cb \le cb_{cr}$, and the slope state reaches the critical state. In this case, the ratio of the actual friction coefficient or connection strength to the critical friction coefficient or connection strength can be taken as the safety factor. Therefore, the slope safety factor can be defined as follows:

(a) (b)

Figure 1: S-RM with an oversized rock block (a) in the diluvium and (b) in the moraine.

Table 1: Mesoscopic mechanical parameters of the soil.

Parameters	Description	Values
ρ	Particle density (kg/m^3)	2160
R_{max}	Maximum particle radius (m)	0.6
R_{max}/R_{min}	Particle radius ratio, uniform distribution	2
k_n	Normal contact stiffness (MPa)	20
k_n/k_s	Normal-to-shear stiffness ratio	2
F_t^c	Tensile strength (kN)	3
F_s^c	Shear strength (kN)	3
μ	Friction coefficient (ball-ball/ball-rock)	0.12

$$SF = \frac{\mu}{\mu_{cr}} = \frac{cb}{cb_{cr}}. \quad (1)$$

2.4. Slope Modeling of S-RMs. The dimensions of the slope model are shown in Figure 2. The slope height is 15 m, and the slope gradient is 1 (vertical):0.56 (horizontal). The concepts of "soil" and "rock" in an S-RM are relative; here, "soil" refers to material with a finer matrix than rock blocks, and there exists a soil/rock threshold distinguishing "soil" from "rock blocks." Grains greater than the threshold size are considered "rock blocks," while grains smaller than the threshold size are defined as "soil" [1]. Medley and co-workers noted that the characteristic size L_c of the research object is the basis for determining the size range of "rock blocks" [2] and that the soil/rock threshold can be defined as $d_{thr} = 0.05\,L_c$, where d_{thr} is the soil/rock threshold of the S-RM and L_c is the height of the slope [29] (L_c is set to 15 m in this study). The size of a rock block is generally 0.75–2 m, and previous studies have shown that a rock block size greater than 0.2 L_c ($0.2L_c$ = 3 m) can be called an oversized rock block [30]. Therefore, in this paper, the size of the oversized rock blocks is set to 3.5 m, the shape of the blocks is set to 4–8 sides, the ratio of the longest and shortest axes of the blocks is set to 1 : 1~1 : 1.5, the blocks are placed randomly in the slope, and the gravity acceleration is 1.0 g. To compare different slope sliding characteristics at the same time, the same calculation time is set for all slopes. According to the trial calculation of the slope, the time is set to 6 s.

According to the structural characteristics of the rock blocks, the spatial distribution of oversized rock blocks has a great impact on the S-RM slope stability. Some scholars have used finite element simulation results to show that the S-RM slope can be mainly divided into three areas: slope toe, slope middle, and slope top (I, II, and III, respectively) [41]. In addition, research shows that the stability of a slope is often dominated by one or more locked segments [42]; therefore, oversized rock blocks are set near the potential slip zone in this paper. As shown in Figure 3, S-RM slope models with RBPs of 10%, 20%, 30%, 40%, and 50% are established. The rock block parameters of each model are the same, while the oversized rock blocks are distributed in areas I, II, or III. Each model contains two oversized rock blocks: R1 and R2. Therefore, the two oversized rock blocks at the slope toe are numbered I-R1 and I-R2, the slope middle blocks are numbered II-R1 and II-R2, and the slope top blocks are numbered III-R1 and II-R2.

3. Analysis of Numerical Results

3.1. Safety Factor Analysis. The safety factors of the S-RM slope with different RBPs are shown in Figure 4, and the relevant statistical results are shown in Table 2, where the average factor of safety is $\overline{X} = \sum_{i=1}^{n} X_i/n$ and the standard deviation is $\sigma = \sqrt{(\sum (X_i - \overline{X})^2/n)}$ (n = 3). The results show that when the oversized rock blocks are located at the toe of the slope, the safety factor of the slope increases significantly with increasing RBP (black spot in Figure 4). When the oversized rock blocks are located at the middle and top of the slope, there is an obvious difference in slope stability at the foot of the slope. When the RBP is less than 30%, the safety factor of the S-RM slope is even smaller than that of the homogeneous soil slope (RBP = 0%) (green triangle and red dot in Figure 4), which shows that in the slope with a low RBP, the existence of oversized rock blocks in the middle and top of the slope is unfavourable to the stability of the slope. This is because when the RBP is low, the rock blocks are fully embedded in the soil, the rock blocks cannot contact each other and provide support, and the density of the rock blocks

Figure 2: The size of the slope model and calculation result of the homogeneous soil slope.

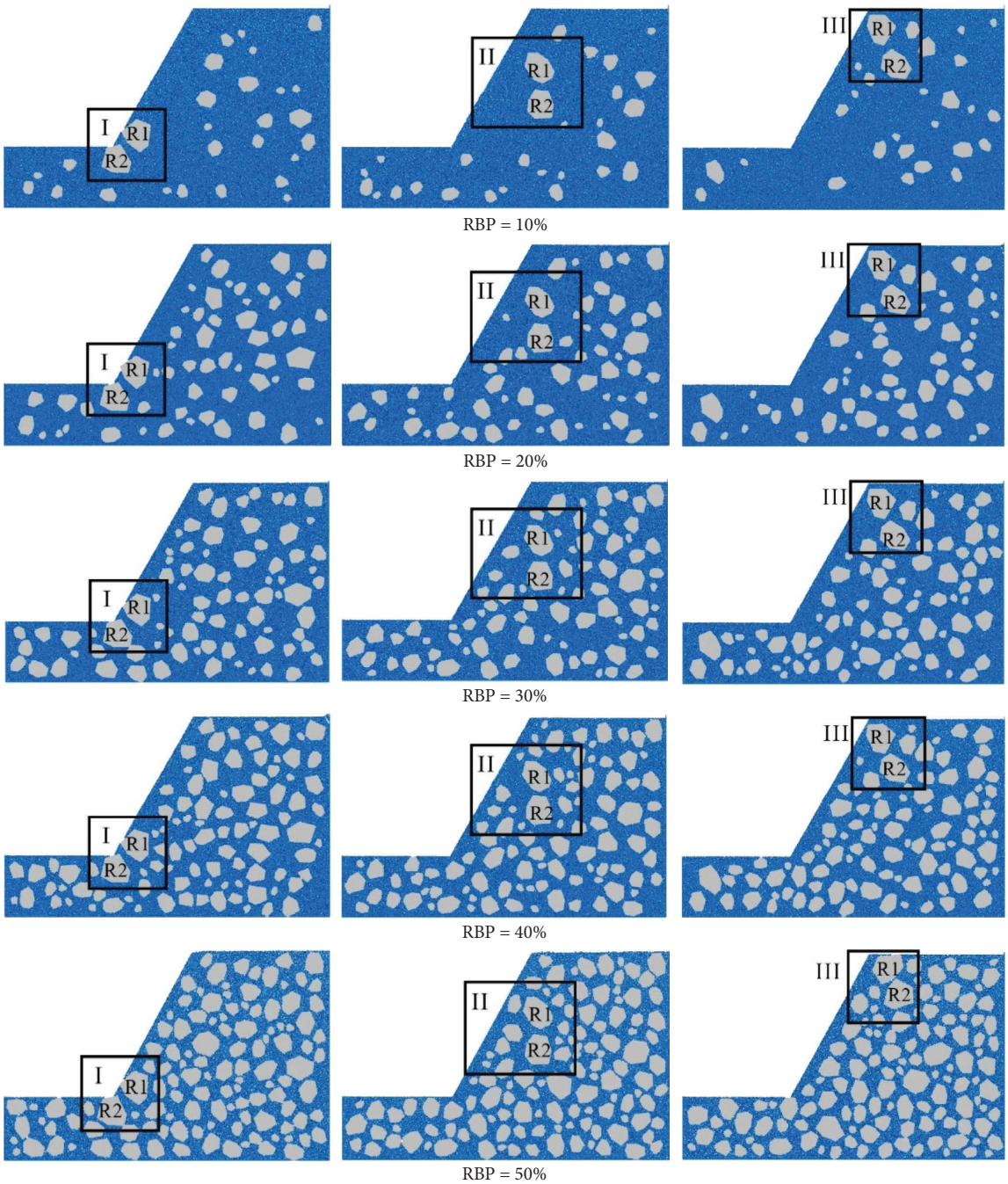

Figure 3: Numerical model of S-RM slopes with different spatial distributions of oversized rock blocks.

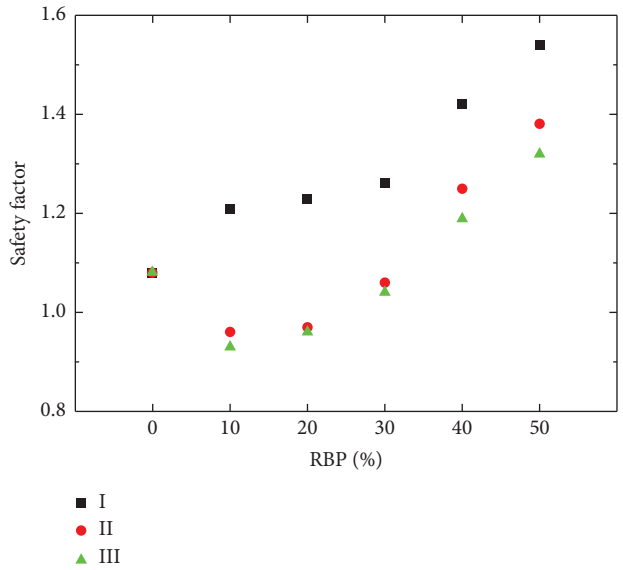

Figure 4: Safety factor of the slope with different spatial distributions of the oversized rock blocks.

Table 2: The safety factor, standard deviation, and coefficient of variation results.

RBP (%)	Spatial distribution characteristics	Safety factor (SF)		
		Calculated value (X_i)	Average value ($\overline{X}$)	Standard deviation (σ)
0	—	1.08	1.08	0.0000
10	I	1.21	1.03	0.1255
	II	0.96		
	III	0.93		
20	I	1.23	1.05	0.1250
	II	0.97		
	III	0.96		
30	I	1.26	1.12	0.0993
	II	1.06		
	III	1.04		
40	I	1.42	1.29	0.0974
	II	1.25		
	III	1.19		
50	I	1.54	1.41	0.0929
	II	1.38		
	III	1.32		

is greater than that of the soil, weakening the strength of the soil in the slope. This result corresponds to the research results of Lu et al. [5], but the RBPs tested in this paper are relatively low because the slope model has a large slope gradient; slope research is an ongoing process, and the slope gradient is also an important factor affecting the S-RM slope.

Regarding the degree of dispersion in the safety factor results (Table 2), when RBP = 10%, the standard deviation of the safety factor is 0.1255, while when the RBP increases to 50%, the standard deviation of the safety factor decreases to 0.0929, which indicates that the dispersion degree of the safety factor decreases with increasing RBP, that is, the impact of the spatial distribution of the oversized rock blocks in the slope on the safety factor gradually decreases with increasing RBP. At the same time, with a low RBP, the safety factor of the slope with the oversized rock blocks at the slope toe is significantly greater than that with the oversized rock blocks in the middle and top of the slope. With the increase in RBP, although the safety factor of the slope with the oversized rock blocks at the slope toe is greater than that with the oversized rock blocks in the middle and top of the slope, the influence of rock blocks on the stability of the slope gradually decreases, which indicates that under the condition of a low RBP, the random spatial distribution of the rock blocks has the greatest influence on the stability of the S-RM slope.

3.2. Sliding Characteristic Analysis. Figure 5 shows the sliding displacement results of the S-RM slopes after calculation. Due to the existence of rock blocks, the potential sliding surface is not a smooth circular surface but rather

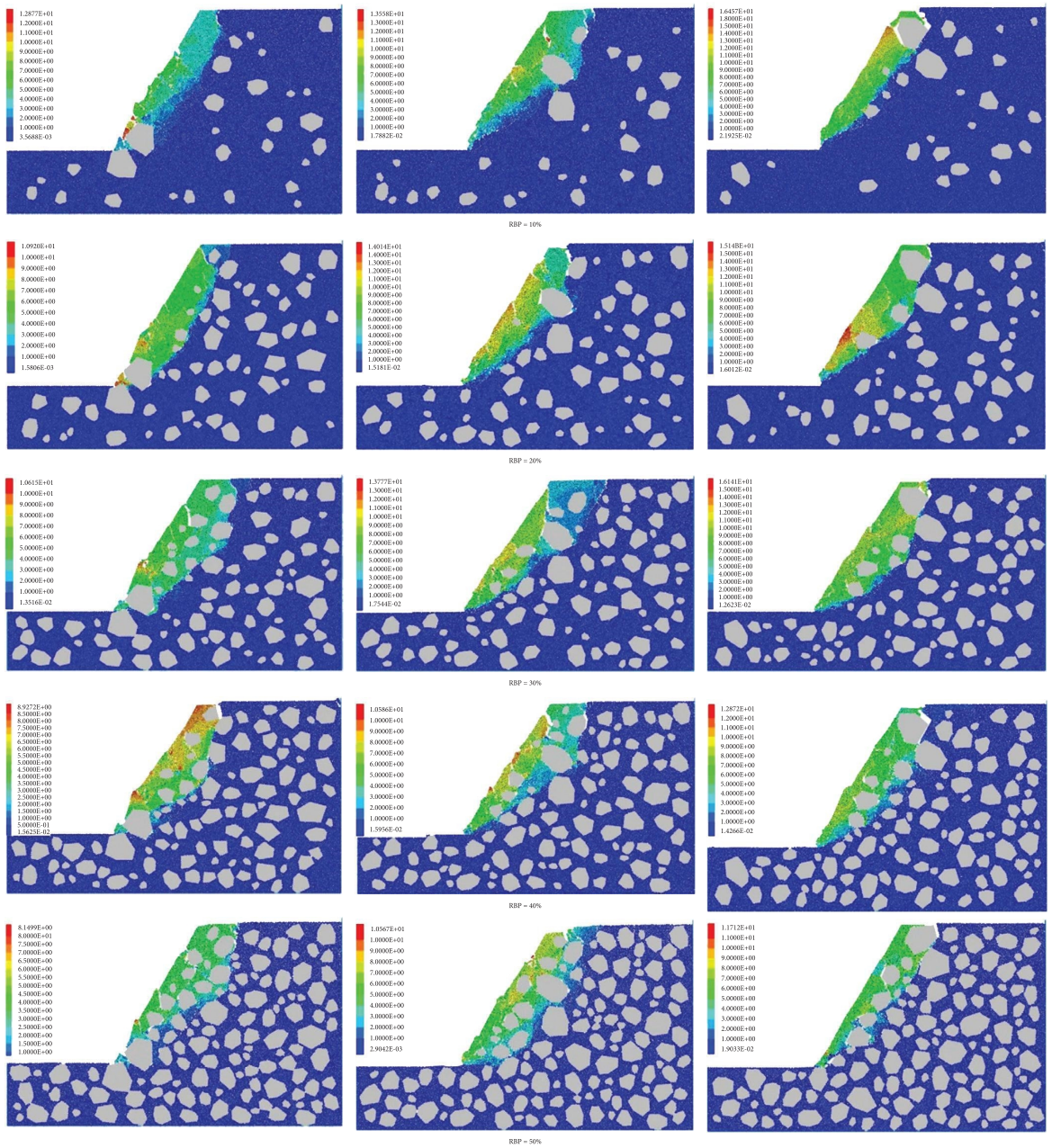

Figure 5: Slope displacement with different spatial distributions of oversized rock blocks.

a tortuous surface. When the RBP in the slope is consistent, the slope displacement with the oversized rock blocks at the slope toe is the smallest, which is due to the good stability of the rock block at the slope toe forming the presser foot effect. When the oversized rock blocks are distributed in the middle of the slope, the scale of the potential sliding body is larger than that with the oversized rock blocks at the slope toe and slope top. The simulation results of this study intuitively show that oversized rock blocks are more likely to rotate when they are located in the middle of the slope, resulting in larger-scale soil sliding, which will be further analysed in the study of the rotation characteristics of oversized rock blocks.

3.3. Unbalanced Contact Force of Oversized Rock Block Analysis. The force of oversized rock blocks in the slope can be revealed from the contact force characteristics, and the unbalanced contact force of the rock blocks can reflect the internal movement of these blocks and their role in the deformation and failure process of the slope [43]. Figure 6 shows the average unbalanced contact force of oversized rock blocks in different slope models. When the oversized rock blocks are located at the toe and top of the slope, the unbalanced force of the oversized rock blocks continues to decrease with the increase in RBP because other rock blocks in the slope also participate in the antisliding effect of the slope.

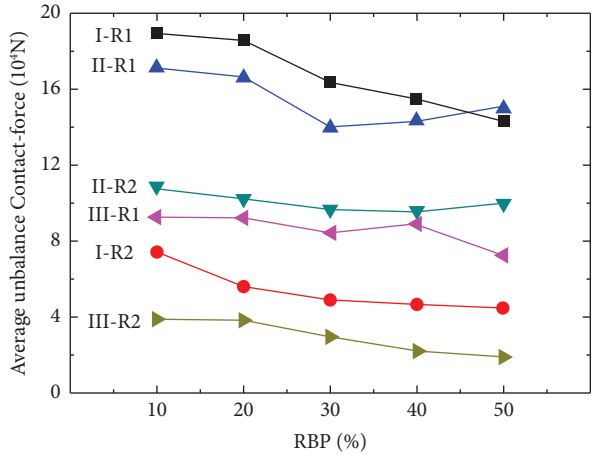

Figure 6: Unbalanced contact forces of the oversized rock blocks.

When the oversized rock blocks are located at the toe of the slope, rock block I-R1 is located in the sliding surface of the slope. For the slope to slide, it first needs to overcome the blocking effect of the rock block, so the unbalanced force on I-R1 is the largest. Rock block I-R2 is located at the toe of the slope and below the sliding surface, so the unbalanced force is low, and only a small fluctuation arises in the calculation process. When the oversized rock blocks are located in the middle of the slope, with the increase in RBP, the unbalanced force on rock blocks II-R1 and II-R2 first decreases and then increases; when RBP <30%, the unbalanced force can be gradually eliminated by the rock block through its own displacement, and with the increase in RBP >30%, the compressible scale of the soil between the rock blocks is small, leading to the strong interaction between blocks and thus the increase in the unbalanced force. The unbalanced force of rock block II-R2 is smaller than that of rock block II-R1. Figure 5 shows that only a small part of rock block II-R2 is near the sliding surface and thus plays a small role in hindering sliding, so the corresponding unbalanced force is also small. When the oversized rock blocks are located at the top of the slope, the unbalanced forces of the oversized rock blocks are small, but the unbalanced force of rock block III-R1 is slightly larger than that of block III-R2. This is because rock block III-R1 is above the sliding surface and undergoes sliding movement under the action of the unbalanced force, while rock block III-R2 is below the sliding surface and cannot eliminate the unbalanced force through its own movement.

The unbalanced forces on the oversized rock blocks at the foot of the slope are the largest, indicating that the rock blocks at the foot of the slope contribute the most to the antisliding of the slope, followed by those at the middle and top of the slope. According to the relative positions of the sliding surface and the oversized rock blocks, the unbalanced forces of the oversized rock blocks within the sliding surface are larger than those farther from the sliding surface. This is because the rock blocks near the sliding surface need to reduce the unbalanced force through their own rotation, which is similar to the function of an antislide pile, and the oversized rock blocks above the sliding surface can overcome the unbalanced force through free movement.

3.4. Rotation Characteristics of Oversized Rock Block Analysis. The rotation of rock blocks is the result of the sliding shear force, and the difference in the shear stress often results in a considerable difference in the rotation of the rock blocks among different areas [44]. This localized difference is an important metric of the local deformation characteristics and is an important reflection of the evolution of the shear zone. In the process of slope sliding, the rotation angles of the oversized rock blocks around their centres of mass are recorded. The rotation amount is expressed in radians. Anticlockwise rotation is positive and clockwise rotation is negative. Figure 7 shows the rotation characteristics of the rock blocks in the slope at the end of the calculation. The rock block rotation mainly occurs near the sliding surface, and the rock blocks below the sliding surface basically do not rotate, which shows that in the sliding process, the sliding shear force on rock blocks is the largest for those near the sliding surface. Among the rotation angles of the oversized rock blocks, those of I-R1 and II-R1 are the largest, and the rotation angles of other oversized rock blocks are not obvious due to the small sliding force and shear force; therefore, only I-R1 and II-R1 are shown in Figure 8.

When the oversized rock blocks are located at the foot of the slope, the rotation angle of rock block R1 at the sliding surface is the largest, indicating that it has the strongest shear force, which is consistent with the unbalanced force characteristics of the oversized rock blocks. In addition, with the increase in RBP (Figure 8), the rotation angle of oversized rock block R1 gradually decreases because other blocks in the slope contribute to the sliding resistance of the slope with the increase in RBP. When the oversized rock blocks are located in the middle of the slope, the rotation angle of rock block R1 at the sliding surface is the largest, indicating that the shear force is also the strongest. The results show that the rotation angle of R1 first decreases and then increases with increasing RBP (minimum at RBP = 30%), which is consistent with the change in the unbalanced contact force. The model results intuitively show that when the RBP is greater than 30%, oversized rock block R1 is supported by R2 and the soil in the middle of the landslide is soft.

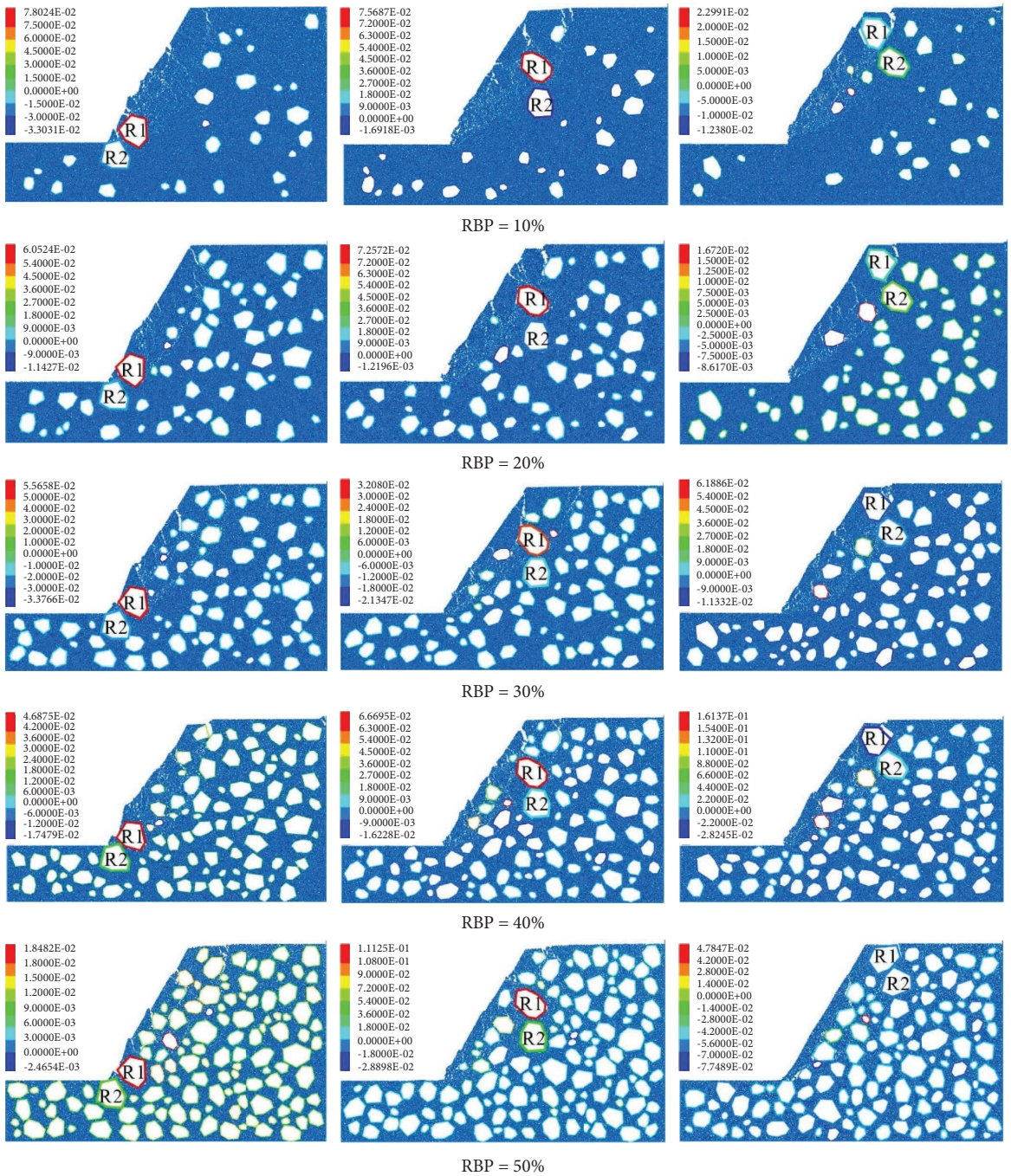

Figure 7: The rotation angle of each rock block with different RBPs.

Therefore, rock block R1 is more prone to toppling and rotation under this condition, resulting in large-scale soil sliding. When the oversized rock blocks are located at the top of the slope, the rotation angles of the rock blocks are small and vary. Figure 7 intuitively shows that the behaviour of the oversized rock blocks changes with position in the slope. This is because the soil near the sliding surface has difficulty restraining the rock block at the trailing edge of the landslide and should not produce shear force. Therefore, the rock block slides with the soil and is difficult to support.

Therefore, in different parts of the slope, the rock blocks are subject to different shear effects, the shear effect of the rock blocks at the foot of the slope is the most obvious, the rock blocks at the slip zone in the middle of the slope are also controlled by the shear effect, and the rock blocks at the top of the slope are basically not subject to a shear force. This shows that only the rock blocks at the foot of the slope play a supporting role in the stability of the slope, whereas those at the sliding zone at the top of the slope cannot. According to direct shear test results, most scholars believe that the rock blocks near the shear

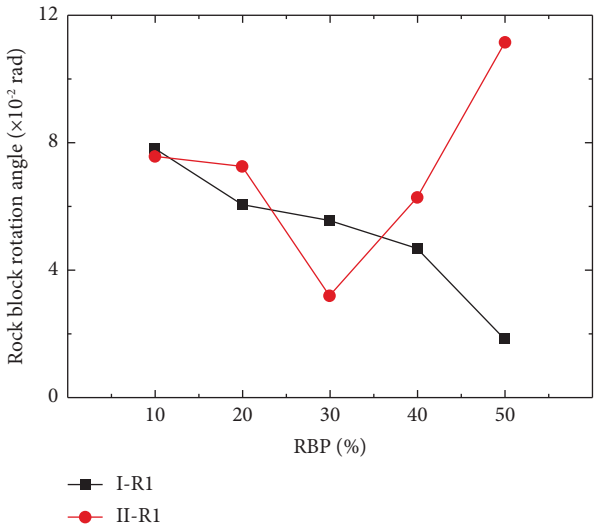

Figure 8: The rotation angles of oversized rock blocks (I-R1 and II-R1) with varying RBPs.

zone have the same mechanical properties as the S-RM [44]. However, the positions of the rock blocks in the slope control the forces acting on them.

4. Discussion

Compared with those of homogeneous soil, the mechanical properties of S-RM are complex due to the existence of rock blocks. For S-RM slopes, because their internal geological structure is difficult to obtain, simplified geological body models or parameters calculated by field tests are often used for stability prediction, which may cause large errors between the prediction results and the actual situation [28]. The numerical simulation results of this paper suggest that the spatial distribution of oversized rock blocks has a significant impact on the stability of the S-RM slope. The slope can be divided into the slope toe, slope middle, and slope top, as shown in Figure 9. The results of shear tests on S-RM suggest that only the rock blocks near the sliding surface control the slope structure [1, 44]. Considering the concept of locked segments [42], we propose the concept of key rock blocks in an S-RM slope. When the potential sliding surface of the S-RM slope lies along oversized rock blocks with high strength, they can bear a considerable stress concentration and generally control the large-scale geometric characteristics and shear stress of the sliding surface. The key rock blocks located at the foot of the slope (zone I) can improve the stability of the slope, while the influence of the key rock blocks located in the middle of the slope (zone II) and at the top of the slope (zone III) on the stability of the slope is related to factors such as RBP, which needs to be further studied.

In addition, the clump algorithm chosen to generate rock blocks in this paper does not allow the rock blocks to deform or break. In practice, a shear force large enough to cut the rock blocks in an S-RM slope may arise [30]. Therefore, the influencing factors of rock block strength should be further studied.

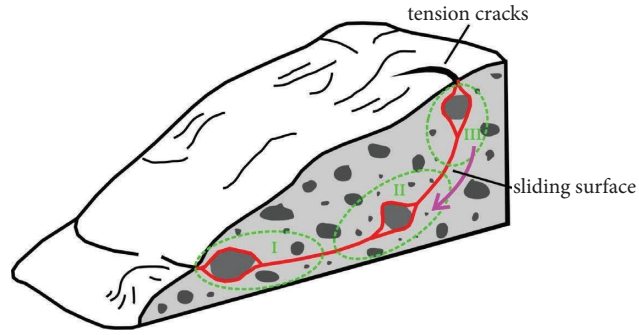

Figure 9: Schematic drawing of the distribution of key rock blocks.

5. Conclusions

Based on the structural characteristics of rock blocks, this paper establishes a slope model of an S-RM with the spatial distribution characteristics of different oversized rock blocks to study the deformation, failure, and stability of the slope. The main conclusions are as follows:

(1) When the oversized rock blocks are located at the foot of the slope, the safety factor of the slope increases significantly with increasing RBP. In slopes with a low RBP, the existence of rock blocks in the middle of the slope and at the top of the slope is unfavourable to the stability of the slope.

(2) The unbalanced contact force of the oversized rock blocks at the foot of the slope is the largest, followed by that at the middle of the slope, and that at the top of the slope is the smallest. According to the relative positions of the sliding surface and the oversized rock blocks, the unbalanced contact force of the oversized rock blocks at the sliding surface is greater than that farther from the sliding surface because the oversized rock blocks near the sliding surface behave similarly to an antislide pile, and the oversized rock blocks above the sliding surface can overcome the unbalanced force through free movement.

(3) The rotation of oversized rock blocks in an S-RM slope occurs mainly near the sliding surface, and the deep rock blocks basically do not rotate. When the oversized rock blocks are located at the foot of the slope, the rotation angle of rock block R1 on the sliding surface is the largest, indicating that the shear force is the strongest. When the oversized rock blocks are located at the top of the slope, the rotation angles are small and vary.

(4) According to the simulation results, the concept of key rock blocks is proposed, which refers to oversized rock blocks with high strength under conditions of stress concentration in the potential sliding surface of an S-RM slope. A key rock block at the foot of the slope can improve the stability of the slope, while the influence of key rock blocks at the middle and top of the slope on the stability of the slope is

related to factors such as RBP, which needs to be further studied.

(5) In addition, it should be specially noted that this paper mainly carries out simulation research on a slope of S-RM containing oversized rock blocks, and the conclusion only applies to certain case-specific conditions. At present, only the influence of the spatial distribution of oversized rock blocks on the S-RM slope is considered. To simulate the deformation and failure mechanism of the S-RM slope more accurately, further research can be considered from the aspects of rock block direction, rock block size, soil and rock bond strength, etc.

Data Availability

The data used to support the findings of this study are included within the article.

Conflicts of Interest

The authors declare that they have no conflicts of interest.

Authors' Contributions

WG contributed to conceptualization, methodology, simulation, data duration, writing the original draft, and funding acquisition. HY contributed to conceptualization, writing, reviewing, and editing, and supervision. JT contributed to data curation, reviewing, and editing. YS contributed to methodology and funding acquisition.

Acknowledgments

The authors are grateful to Dr. Xueyun Wei, professor of College of Architecture Engineering, Quzhou University, Quzhou, for her great help and valuable discussions on this work. This work was supported by the Natural Science Basic Research Program of Shaanxi (Grant no. 2021JQ-632), the National Natural Science Foundation of China (Grant no. 42007238), and the Scientific Research Project of Yan'an University (Grant no. YDBK2019–37). The authors greatly appreciate this financial support.

References

[1] D. F. Cen, D. Huang, and F. Ren, "Shear deformation and strength of the interphase between the soil-rock mixture and the benched bedrock slope surface," *Acta Geotechnica*, vol. 12, no. 2, pp. 391–413, 2017.

[2] E. W. Medley, *The engineering characterization of melanges and similar block-in matrix rocks (bimrocks)*, Ph.D. thesis, University of California, Berkeley, CA, USA, 1994.

[3] W. J. Xu, L. M. Hu, and W. Gao, "Random generation of the meso-structure of a soil-rock mixture and its application in the study of the mechanical behavior in a landslide dam," *International Journal of Rock Mechanics and Mining Sciences*, vol. 86, pp. 166–178, 2016.

[4] L. J. West, S. R. Hencher, and T. W. Cousens, "Assessing the stability of slopes in heterogeneous soils," *European Online Journal of Natural and Social Sciences*, vol. 3, no. 4, 1992.

[5] Y. Lu, Y. Tan, and X. Li, "Stability analyses on slopes of clay-rock mixtures using discrete element method," *Engineering Geology*, vol. 244, pp. 116–124, 2018.

[6] X.-W. Huang, Z.-S. Yao, W. Wang, A.-Z. Zhou, and P. Jiang, "Stability analysis of soil-rock slope (SRS) with an improved stochastic method and physical models," *Environmental Earth Sciences*, vol. 80, no. 18, p. 649, 2021.

[7] W. Gao, H. Yang, and R. Hu, "Soil–rock mixture slope stability analysis by microtremor survey and discrete element method," *Bulletin of Engineering Geology and the Environment*, vol. 81, no. 3, p. 121, 2022.

[8] X. Li, Q. Liao, and J. He, "In situ tests and a stochastic structural model of rock and soil aggregate in the Three Gorges reservoir area, China," *International Journal of Rock Mechanics and Mining Sciences*, vol. 41, no. 3, p. 494, 2004.

[9] T. Irfan and K. Tang, "Effect of the coarse fraction on the shear strength of colluvium in Hong Kong," *Hong Kong Geotechnical Engineering office Report*, vol. 4, p. 92, 2002.

[10] S. Mahdevari and P. Maarefvand, "Applying ultrasonic waves to evaluate the volumetric block proportion of bimrocks," *Arabian Journal of Geosciences*, vol. 10, no. 9, pp. 204–212, 2017.

[11] E. Medley, "Uncertainty in estimates of block volumetric proportion in melange bimrocks," in *Proceedings of the International Symposium on Engineering Geology and the Environment Balkema*, pp. 267–272, Rotterdam, The Netherlands, December 1997.

[12] S. Wang, Y. Li, X. Gao, Q. Xue, P. Zhang, and Z. Wu, "Influence of volumetric block proportion on mechanical properties of virtual soil-rock mixtures," *Engineering Geology*, vol. 278, Article ID 105850, 2020.

[13] M. Afifipour and P. Moarefvand, "Mechanical behavior of bimrocks having high rock block proportion," *International Journal of Rock Mechanics and Mining Sciences*, vol. 65, pp. 40–48, 2014.

[14] E. S. Lindquist, *Strength and deformation properties of melange*, Ph.D. thesis, University of California, Berkeley, CA, USA, 1994.

[15] M. L. Napoli, M. Barbero, E. Ravera, and C. Scavia, "A stochastic approach to slope stability analysis in bimrocks," *International Journal of Rock Mechanics and Mining Sciences*, vol. 101, pp. 41–49, 2018.

[16] S. Liu, H. Wang, W. Xu, Z. Cheng, Z. Xiang, and W.-C. Xie, "Numerical investigation of the influence of rock characteristics on the soil-rock mixture (SRM) slopes stability," *KSCE Journal of Civil Engineering*, vol. 24, no. 11, pp. 3247–3256, 2020.

[17] M. Barbero, M. Bonini, and M. Borri-Brunetto, "Numerical simulations of compressive tests on bimrock," *Electronic Journal of Geotechnical Engineering*, vol. 17, pp. 3397–3414, 2012.

[18] Y. Wang, *Research on the Mechanical Behavior of Rock and Soil Aggregates Based on Meso-Structural Mechanics*, Institute of Geology and Geophysics, Chinese Academy of Science, Beijing, China, 2014.

[19] Y. Liang, L. Cao, J. Liu, and W. Sui, "Numerical simulation of mechanical response of glacial tills under biaxial compression with the DEM," *Bulletin of Engineering Geology and the Environment*, vol. 78, no. 3, pp. 1575–1588, 2019.

[20] L. Chen, Y. Yang, and H. Zheng, "Numerical study of soil-rock mixture: generation of random aggregate structure," *Science China Technological Sciences*, vol. 61, no. 3, pp. 359–369, 2018.

[21] H. Xianwen, Y. Zhishu, and W. Wei, "Stability analysis of the soil–rock slope considering long axis inclination and soil–rock interface," *Advanced Engineering Sciences*, vol. 53, no. 1, pp. 47–59, 2021.

[22] E. S. Lindquist and R. E. Goodman, *Strength and Deformation Properties of A Physical Model Melange*, OnePetro, Richardson, TX, USA, 1994.

[23] A. Kalender, H. Sonmez, E. Medley, C. Tunusluoglu, and K. E. Kasapoglu, "An approach to predicting the overall strengths of unwelded bimrocks and bimsoils," *Engineering Geology*, vol. 183, pp. 65–79, 2014.

[24] Y. Wang, X. Li, B. Zheng, B. Zhang, J. He, and S. Li, "Macro–meso failure mechanism of soil–rock mixture at medium strain rates," *Géotechnique Letters*, vol. 6, no. 1, pp. 28–33, 2016.

[25] S. Zhang, H. Tang, H. Zhan, G. Lei, and H. Cheng, "Investigation of scale effect of numerical unconfined compression strengths of virtual colluvial-deluvial soil-rock mixture," *International Journal of Rock Mechanics and Mining Sciences*, vol. 77, pp. 208–219, 2015.

[26] N. Casagli, L. Ermini, and G. Rosati, "Determining grain size distribution of the material composing landslide dams in the Northern Apennines: sampling and processing methods," *Engineering Geology*, vol. 69, no. 1-2, pp. 83–97, 2003.

[27] W. J. Xu, *Study on Meso-Structural Mechanics (M-sm) Characteristics and Stability of Slope of Soil –rock Mixtures (S-rm)*, Institute of Geology and Geophysics, Chinese Academy of Science, Beijing, China, 2008.

[28] S. Shao and S. Ji, "Effects of rock spatial distributions on stability of rock-soil- mixture slope," *Engineering Mechanics*, vol. 31, no. 2, pp. 177–183, 2014.

[29] W. Gao, W. Gao, R. Hu, P. Xu, and J. Xia, "Microtremor survey and stability analysis of a soil-rock mixture landslide: a case study in Baidian town, China," *Landslides*, vol. 15, no. 10, pp. 1951–1961, 2018.

[30] J. Xia, R. Hu, S. Qi, W. Gao, and H. Sui, "Research on large-scale triaxial shear testing of soil rock mixtures containing oversized particles," *Chinese Journal of Rock Mechanics and Engineering*, vol. 36, no. 8, pp. 2031–2039, 2017.

[31] P. A. Cundall, *PFC2D Theory and Background*, Itasca Consulting Group, Minneapolis, MN, USA, 2004.

[32] C. Shi and W. Xu, *Numerical Simulation Skills and Practice of Particle Flow Code (PFC)*, China Architecture and Building Press, Beijing, China, 2015.

[33] W. Gao, H. Yang, L. Wang, and R. Hu, "Numerical simulations of the soil–rock mixture mechanical properties considering the influence of rock block proportions by PFC2D," *Materials*, vol. 14, no. 18, p. 5442, 2021.

[34] Z. Yang, X. Lei, L. Wang, Y. Hu, and Y. Liu, "Impact of stone content to shear properties of soil-rock mixture using particle flow code simulation," *Journal of Engineering Geology*, vol. 25, no. 4, pp. 1035–1045, 2017.

[35] S. N. Wang, C. Shi, W. Y. Xu, H. L. Wang, and Q. Z. Zhu, "Numerical direct shear tests for outwash deposits with random structure and composition," *Granular Matter*, vol. 16, no. 5, pp. 771–783, 2014.

[36] Y. Zeng, *Microscopic Mechanics of Soil Failure and PFC Numerical Simulation*, Tongji University, Shanghai, China, 2006.

[37] C. Shi, Q. Zhang, and S. N. Wang, *Numerical Simulation Technology and Application with Particle Flow Code (PFC5.0)*, China Architecture and Building Press, Beijing, China, 2018.

[38] J. Ji, H. Cui, T. Zhang, J. Song, and Y. Gao, "A GIS-based tool for probabilistic physical modelling and prediction of landslides: GIS-FORM landslide susceptibility analysis in seismic areas," *Landslides*, vol. 19, no. 9, pp. 2213–2231, 2022.

[39] J. Ji, C. Zhang, Y. Gao, and J. Kodikara, "Reliability-based design for geotechnical engineering: an inverse FORM approach for practice," *Computers and Geotechnics*, vol. 111, pp. 22–29, 2019.

[40] J. Ji, C.-W. Wang, Y. Gao, and L. Zhang, "Probabilistic investigation of the seismic displacement of earth slopes under stochastic ground motion: a rotational sliding block analysis," *Canadian Geotechnical Journal*, vol. 58, no. 7, pp. 952–968, 2021.

[41] S. Liu, X. Huang, A. Zhou, J. Hu, and W. Wang, "Soil-rock slope stability analysis by considering the nonuniformity of rocks," *Mathematical Problems in Engineering*, vol. 2018, Article ID 3121604, 15 pages, 2018.

[42] H. Chen, S. Qin, L. Xue, B. Yang, and K. Zhang, "A physical model predicting instability of rock slopes with locked segments along a potential slip surface," *Engineering Geology*, vol. 242, pp. 34–43, 2018.

[43] L. Jin and Y. Zeng, "Refined simulation for macro-and meso-mechanical properties and failure mechanism of soil-rock mixture by 3D DEM," *Chinese Journal of Rock Mechanics and Engineering*, vol. 37, no. 6, pp. 1540–1550, 2018.

[44] F. Hu, Z. Li, R. Hu, Y. Zhou, and R. Yue, "Research on the deformation characteristics of shear band of soil-rock mixture based on large scale direct shear test," *Chinese Journal of Rock Mechanics and Engineering*, vol. 37, no. 3, pp. 766–778, 2018.